

Project: 620

Project title: Vertical Propagation of Gravity Waves into the Middle Atmosphere

Project lead: Andreas Dörnbrack

Report period: 2022-01-01 to 2023-04-30

During the reporting period, computational time has primarily been used for simulations of deep gravity wave propagation events observed during the SOUTHTRAC GW campaign (Rapp et al., 2021) and the DEEPWAVE 2014 field campaign (Fritts et al., 2016). Published results can be found here: Dörnbrack et al., 2020, Rapp et al., 2021, Mixa et al., 2021. A major part of the computational time went into the master thesis of Michael Binder (Binder, 2023); selected results are presented in the first part of this report.

Stratospheric gravity waves excited by the airflow across a propagating upper-level trough

Idealized numerical simulations with the EULAG model have been conducted to investigate the hypothesis that non-orographic gravity waves are excited by the sheared stratospheric air flow across propagating upper-level troughs associated with eastward propagating Rossby waves. These troughs are represented as tropopause depressions or, literally, as vertically displaced isentropes in the lowermost stratosphere. The non-orographic gravity waves excited by the propagating Rossby waves might contribute significantly to the gravity wave belt observed over the Southern Ocean in the Southern Hemisphere winter stratosphere (Hindley et al., 2020). Based on a case study from the DEEPWAVE field campaign, Dörnbrack et al. (2022) proposed the excitation of non-orographic gravity waves via horizontally propagating, vertically displaced isentropes in the lowermost stratosphere above upper-level troughs, similar to the excitation of orographic gravity waves by tropospheric airflow over mountains. However, the phases of the non-orographic gravity waves are fixed in the reference frame of the upper-level trough associated with the eastward propagating Rossby waves.

This brief report sketches selected main results that are part of the master thesis of Michael Binder. In a first step, non-linear numerical simulations with the EULAG model were conducted to reproduce analytic solutions of the gravity wave drag and surface momentum and energy fluxes for Queney's idealized mountain wave regimes (Queney, 1948) that cover mountain widths from 1 to about 100 km, see Figure 1. The results emphasized the significance of the subsequent simulations with propagating tropopause depressions to cover a broad spectrum of excited gravity waves from non-hydrostatic (i.e., high-frequency) waves to inertia-gravity (i.e. low frequency) waves. The investigations clarified inconsistencies between different linear solutions for the rotating hydrostatic mountain wave regime as published in the literature, compare caption of Figure 1.

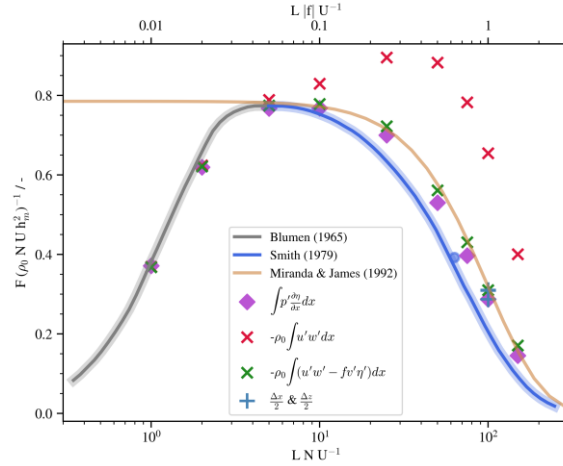


Figure 1: The force F is the gravity wave drag F_x normalized by $\rho_0 N U h_m^2$ for the linear momentum flux of the flow over a Witch of Agnesi with half width L . Thicker faded lines indicate that the linear solution is based on Bessel functions (Blumen, 1965 and Smith, 1979). Miranda and James (1992) provide an analytical solution for the hydrostatic rotating limit (inertia-gravity waves). Buoyancy frequency N and flow speed U are uniform and the Coriolis frequency $f = 0.01N$. Purple hashes represent the simulated gravity wave drag, red crosses the linear momentum flux MF_x and green crosses the angular momentum flux $MF_{x,ang}$ according to formulas provided by Bretherton (1969), Smith (1979), and Broad (1995), respectively, for different mountain wave regimes with varying mountain half width L .

Adopting the proposed excitation mechanism of non-orographic gravity waves above propagating upper-level troughs, all numerical simulations use a transient, impermeable, and frictionless lower boundary to simulate isentropes in the lowermost stratosphere. Thus, all numerical simulations were limited to the airflow in the stratosphere, and it was appropriate to assume a purely zonal ambient airflow for the idealized investigations.

Under these assumptions, a fundamental result is that increasing (decreasing) the ambient wind $u_e(z)$ by a constant speed c_{ef} (the phase speed of the propagating upper-level trough) has a similar effect as decreasing (increasing) their

propagation speed by c_{tf} , see Figure 1. Thus, non-orographic gravity waves above upper-level troughs behave and propagate just like mountain waves within the reference frame of the propagating depression for a relative ambient wind $u_e(z)$. Furthermore, it could be shown that a local wind minimum in the vertical profile $u_e(z)$ constrains the gravity wave activity to a zonally narrower region above the upper-level trough (not shown here). In the presence of this so-called valve layer, inertia-gravity waves look like non-rotating hydrostatic gravity waves and are very similar to gravity waves in the vertical cross-sections of ERA5 temperature perturbations from the results of Dörnbrack et al. (2022), where the main wave activity is also centered directly above the upper-level trough.

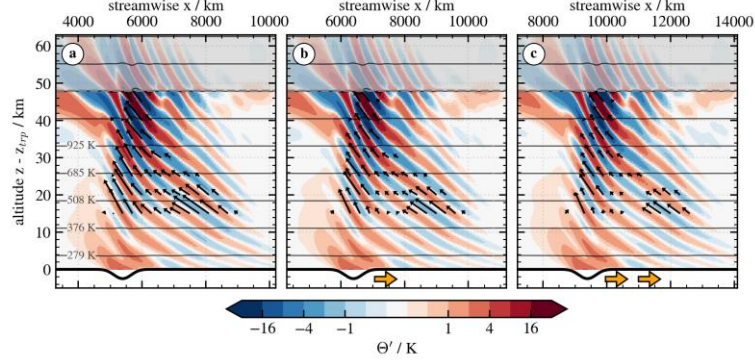


Figure 2: Potential temperature perturbations Θ' overlaid by normalized vectors of wave energy flux \mathbf{EF} for three different simulations with a constant background wind profile u_e that corresponds to a $u_{e,MW} = 31.12 \text{ m s}^{-1}$. (a) represents the “mountain wave case” with a stationary lower boundary. In (b) the tropopause fold moves with c_{tf} and the background wind is increased by c_{tf} . In (c) the upper-level trough moves with $2 c_{tf}$ and again the background wind is increased by $2 c_{tf}$ with respect to (a). Note the different positions of the tropopause fold in streamwise direction after $t = 60 \text{ h}$ and the strong similarity of the stratospheric wave response in all three simulations. The amplitude of the lower boundary is exaggerated by a factor of 5 and the direction of \mathbf{EF} is adjusted to the horizontal and vertical scales of the axes.

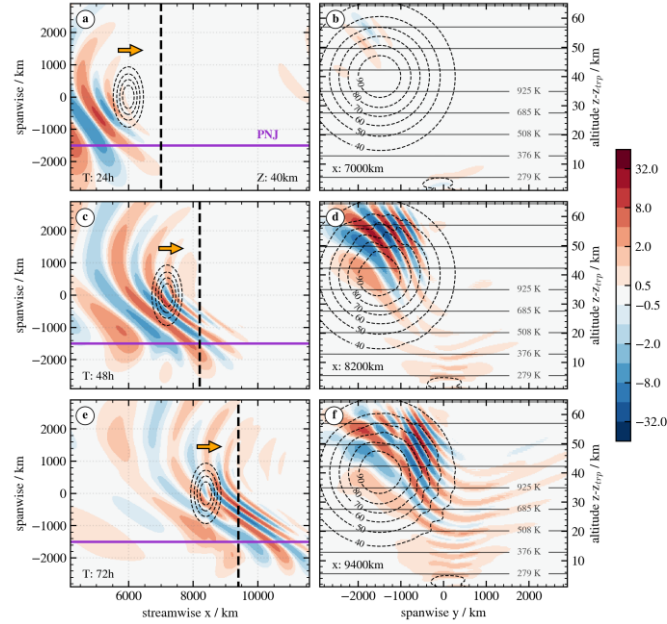


Figure 3: The reference simulation of the entirely 3D simulations with meridional background wind shear. (a), (c) and (e) show horizontal cross sections of Θ' at $z = 40 \text{ km}$ altitude for three times. (b), (d) and (f) show corresponding meridional cross sections 900 km in the lee of the propagating upper-level trough. The position is also indicated in the horizontal cross sections by the dashed black lines. The purple lines in (a), (c) and (e) refer to the location of the polar night jet. Meridional cross sections also show zonal wind u (dashed lines) and isentropes (solid lines).

Numerical simulations of the meridionally sheared stratospheric airflow (due to the presence of a polar night jet, PNJ) across a three-dimensionally shaped upper-level trough demonstrated that excited non-orographic gravity waves propagate vertically and meridionally into the core of the PNJ, see Figure 3. In this way, these results of the idealized numerical simulations confirm the existence of the elongated phase lines found in the horizontal cross-sections of ERA5 temperature perturbations from Dörnbrack et al. (2022). The necessary conditions to obtain such gravity wave patterns are a strong PNJ with its core south of upper-level trough (for the southern hemisphere). In the future, the time-dependent lower boundary in the current simulations will be replaced by a quasi-realistic tropospheric airflow. Here, the upper-level trough will develop during a simulated baroclinic life cycle. This advanced approach allows a more realistic representation of the synoptic conditions in the troposphere over the Southern Ocean and its interaction with the stratospheric airflow.